

Confinement of Pure-Electron Plasmas in a Toroidal Magnetic-Surface Configuration

H. Saitoh,* Z. Yoshida, C. Nakashima, H. Himura, J. Morikawa, and M. Fukao

Graduate School of Frontier Sciences, The University of Tokyo, 7-3-1 Hongo, Bunkyo-ku, Tokyo 113-0033, Japan

(Received 17 February 2003; published 25 June 2004)

A pure-electron plasma has been confined in a toroidal magnetic-surface configuration for as long as classical diffusion time due to neutral collisions. By controlling the potential of the internal conductor, long-term stable confinement of electrons has been achieved in a toroidal geometry.

DOI: 10.1103/PhysRevLett.92.255005

PACS numbers: 52.27.Jt, 52.27.Aj, 52.35.Fp

The magnetic confinement of charged particles has a variety of applications in the fields of atomic physics [1], particle physics (including the study of antimatters [2,3]), as well as plasma physics [4]. The fundamental principle governing the magnetic trapping of a non-neutral plasma is the production of a spontaneous flow of particles in a magnetic field so that the self-electric field is neutralized in the comoving frame. So-called “thermal equilibrium” may be achieved in a homogeneous magnetic field with the help of an appropriate external longitudinal electric field [4,5]. This equilibrium is considered to be a relaxed state under the constraint of the canonical angular momentum of the rotation flow.

The use of toroidal geometry allows us to remove the “open ends” of magnetic field lines and the plugging electric fields. It thus becomes possible to trap high-energy beam particles or to confine multiple species of different charges. Studies regarding pure toroidal magnetic fields [6–13] have revealed an interesting equilibrium state; one is in marked contrast to the confinement of a neutral plasma, which requires twists (rotational transforms) of magnetic field lines in order to avoid the drift loss of particles. However, the obtained confinement time in the pure toroidal magnetic field configuration so far was limited to around 100 μ s.

Another possibility for the stable confinement of toroidal non-neutral plasmas is the use of poloidal magnetic fields that may organize a “closed magnetic-surface configuration.” This is the common configuration for the confinement of usual neutral plasmas and is also a natural extension of the above-mentioned thermal equilibrium under the constraint of the canonical momentum [14]. Closed magnetic surfaces can be produced by a ring conductor hung in a vacuum vessel or by using a superconducting levitated ring [15]. A helical device is another solution to produce closed magnetic surfaces with only “external” windings [16].

In this Letter, we present the experimental demonstration of the long-term confinement of an electron plasma in a toroidal configuration. In the Proto-RT device [15] (Fig. 1), we may produce a variety of magnetic field configurations by superposing dipole, vertical, and toroidal magnetic fields. The electric potentials of the ring conductor and the center stack are controlled in order to alter

the electric field configuration [17]. We have confirmed long-term stable confinement under an appropriate control of the electric field. The obtained confinement time is subsecond order, and it is comparable to the classical diffusion time due to collisions with residual neutral gas in the present experiment.

The chamber of the Proto-RT has a rectangular poloidal cross section of 90 cm \times 53.3 cm and is pumped to a base pressure of 8×10^{-5} Pa. Toroidal field coils are assembled in a center stack (CS) of 11.4 cm diameter. A ring-shaped internal conductor (IC) producing a dipole magnetic field, used in this experiment, is hung by support rods connected to the CS. Electric current and freon coolant are fed through a pair of tube structures via the CS. Vertical field coils are installed outside the chamber. As an initial experiment, we used a dipole magnetic field configuration. The IC coil current fed by a dc power source is 10.5 kAT and the typical magnetic field strength is of order 10^{-2} T. All structures intersecting the plasma confinement region are covered by ceramics. Electrodes (1 mm thick stainless steel) are mounted on the IC and the CS are power fed by a dc power source of 350 V, for the

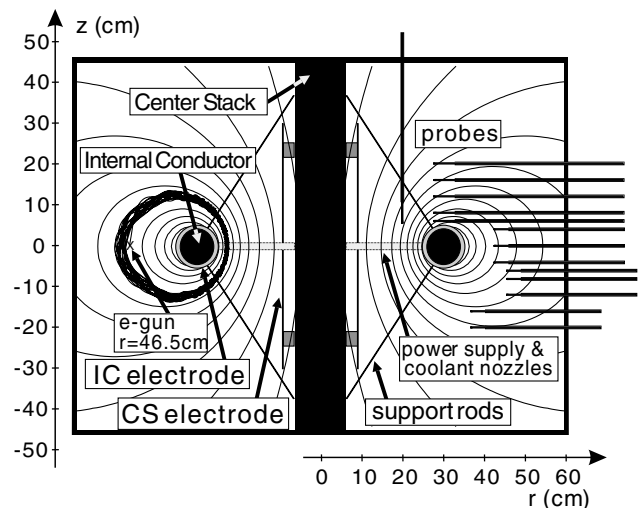


FIG. 1. The poloidal cross section of the Proto-RT chamber, the magnetic surfaces of dipole field, and the typical electron orbit after being injected from the electron gun. A pair of vertical field coils (not seen) is located outside of the chamber.

application of controlling electric fields. We inject electrons using an electron gun that is operated at an acceleration voltage of 300 V and is located at $r = 46.5$ cm and $z = 0$. The gun was operated at a base pressure of below 1×10^{-3} Pa to avoid rapid evaporation of the cathode. Because of the large gyration radius, electrons obey a strongly nonlinear equation of motion in the inhomogeneous magnetic field, resulting in chaotic (nonperiodic) motion with long orbit lengths [18]. We can inject electrons effectively from the edge of the confinement region [19]. A typical electron orbit in our geometry is shown in Fig. 1 (projection on the poloidal cross section) and in Refs. [19,20]. Electrons encircle the chamber due to the $\mathbf{E} \times \mathbf{B}$ and $\nabla B/\text{curvature}$ drifts in the toroidal direction. In the present experiments, the electron injection beam current was 26 mA when V_{IC} (IC electrode bias voltage) was 0, and 5.9 mA when $V_{\text{IC}} = -300$ V.

Internal potential distribution was measured using an array of emissive Langmuir probes. The probe tip is a 0.1 mm diameter thoria-tungsten spiral filament. The circuits are terminated by a resistance of 100 M Ω in order to operate probes at floating potentials (ϕ_{HS}). We also studied the probe characteristics (I - V curves) and confirmed that the potential ϕ_H measured by a high-impedance emissive probe is in agreement with the space potential (ϕ_p) within an error of 20%.

Figure 2 shows the structure of the internal electric potential during the electron injection (the injection period was 100 μs). The case in which the IC electrode is grounded is shown in Fig. 2(a). By solving the Poisson equation [17], we may reproduce the measured potential profile, assuming an electron cloud with a peak number density of 1×10^{13} m $^{-3}$ and a total space charge of $3 \times$

10^{-7} C. The high density region is relatively remote from the support rods of the internal conductor throughout the experiments, and this structure does not seriously perturb the electron plasmas. The potential contours in this configuration do not coincide with the magnetic surfaces, implying a rapid particle loss across the field lines. The grounded IC yields a hollow potential, resulting in a strong $\mathbf{E} \times \mathbf{B}$ flow shear that may destabilize the Kelvin-Helmholtz (diocotron) modes.

The potential profile was successfully modified by applying a potential V_{IC} to the electrodes. Figure 2(b) shows the case when $V_{\text{IC}} = -300$ V, the same potential as the acceleration voltage of the electron gun. The negatively biased IC electrode eliminates the hole of the potential, and the contours of the potential approximate the magnetic surfaces. The peak density and total charge are estimated to be 1×10^{13} m $^{-3}$ and 4×10^{-7} C, respectively. In comparison with the previous case, the amplitude of the fluctuations in the probe signals diminished by a factor of 10.

During the electron injection, the loss of electrons through the Langmuir probe was of the order 1 μA . The lifetime of the electron plasma is strongly affected by the insertion of the probes. When the probe tip was located at $R \leq 45$ cm, no stable equilibrium was obtained. Thus the perturbation due to the probing is a serious problem for estimating the confinement time after cutting off the gun injection. For this purpose, we have used wall probes [9] that measure the image charges induced by electron plasmas. A sensor foil (copper sheet of 5 mm \times 15 mm) was installed in an insulating quartz tube and was placed just outside the confinement region. The foil was electrically connected to the chamber

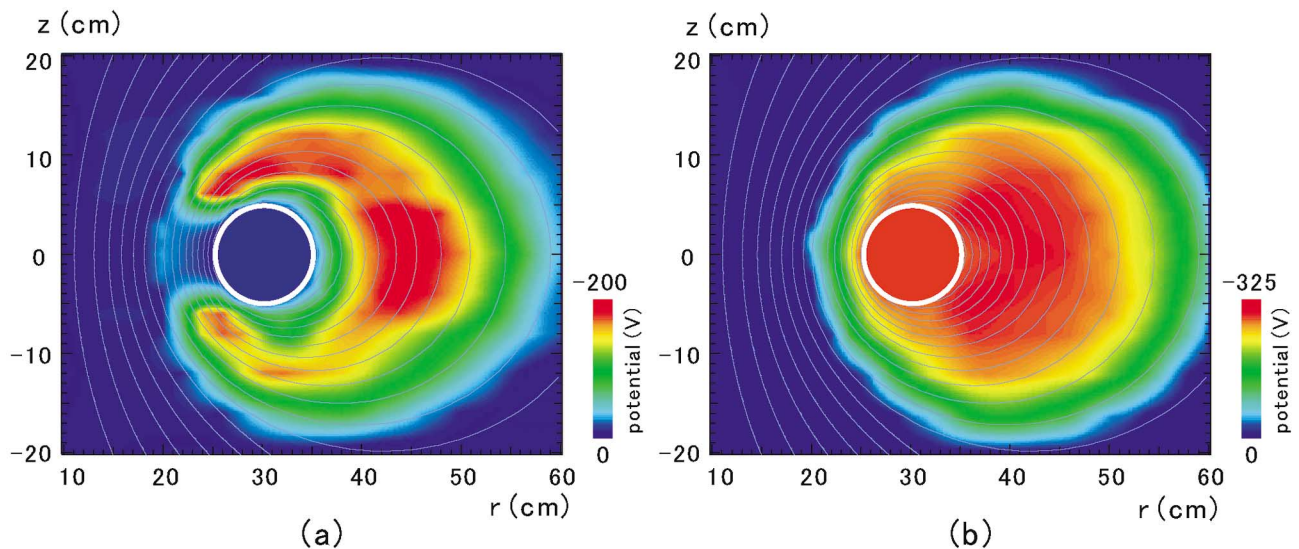


FIG. 2 (color). Potential profiles of an electron plasma in a poloidal cross section of the Proto-RT (a) when the potential is not controlled: IC electrode bias $V_{\text{IC}} = 0$ and (b) when the IC electrode is negatively biased: $V_{\text{IC}} = -300$ V. The profile images are reconstructed from 284 data points measured shot by shot. The thin lines show the magnetic surfaces. Base pressure $P_{\text{base}} = 8 \times 10^{-5}$ Pa and typical magnetic field strength $B_{\text{typ}} = 1.3 \times 10^{-2}$ T.

through a current amplifier, and the image current was measured. Oscillations in the image currents indicate electrostatic fluctuations, giving an evidence for the plasma. In order to evaluate the charge confinement time more explicitly, we destroy the equilibrium by dropping the electrode potential and detecting the escaping image charges.

An example of the detected fluctuations is shown in Fig. 3(a) for the case of negatively biased IC. During the electron injection ($t = -100 \mu\text{s}$ to 0), we observe large, almost coherent amplitude oscillations. The dominant frequency is 510 kHz which corresponds to the diocotron frequency (discussed below). After the electron injection was stopped, the amplitude of the oscillations decreases exponentially with a time constant of $20 \mu\text{s}$, and then, some quiescent periods follow. The stable phases appear when the magnetic field is stronger than $\sim 10^{-2}$ T (measured at the edge of the confinement region) and $V_{\text{IC}} \leq -10^2$ V. The lifetime of the first stable phase is at most 0.4 ms. Near the end of the quiescence, fluctuations grow rapidly. The fluctuations quench again when the frequency drops down to 43 kHz ($t = 0.7$ ms). As shown in Fig. 4, the dominant frequency of the fluctuations is inversely proportional to the magnetic field strength B and also to V_{IC} . The second quiescent phase lasts relatively long at more than 10^{-1} s. The typical time constant of the growth rate of observed fluctuations at the termination phase was $100 \mu\text{s}$. One of the possible reasons for the onset of fluctuations is ion resonance instability caused by the ionization of neutral background gas [21,22]. When the IC electrode is grounded, and thus the initial potential profile does not coincide with the magnetic surfaces, such

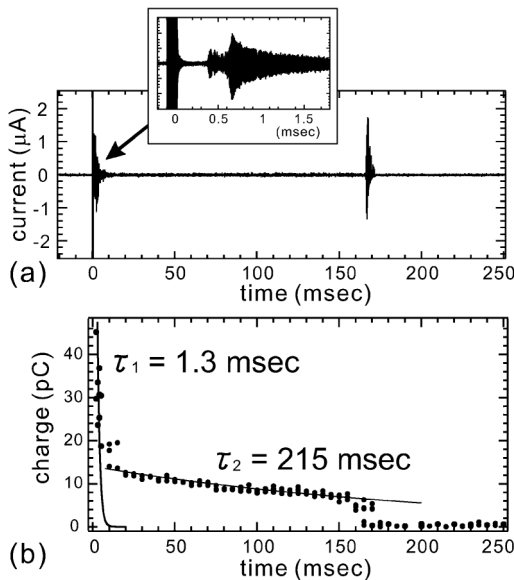


FIG. 3. (a) Waveform of the wall probe signal. (b) Decay of the charge on the wall probe. The IC electrode was biased to -300 V. The gun was terminated at $t = 0$. $P_{\text{base}} = 8 \times 10^{-5}$ Pa and $B_{\text{typ}} = 1.3 \times 10^{-2}$ T.

kinds of long-lasting signals are not observed, and the trapped charge decays away in a time constant of about $10 \mu\text{s}$ after the stop of the electron supply.

Frequency analysis suggests that the observed electrostatic fluctuations are due to the diocotron oscillations. However, a direct correlation between frequency and density cannot easily be drawn, because our system has an inhomogeneous magnetic field and complicated conducting boundaries. Here we borrow the empirical formula for the $l = 1$ diocotron oscillation in a toroidal electron plasma due to Daugherty *et al.* [9], i.e., $f \approx Q/(8\pi^3 R a^2 \epsilon_0 B)$, where Q is the total charge, R (a) is the major (minor) radius of the toroid, ϵ_0 is the vacuum dielectric constant, and B is the magnetic field strength at $r = R$. Then, the total charge is estimated to be $\sim 1 \times 10^{-7}$ C for the electron injection phase. In the geometry of Proto-RT, the large amount (up to $\sim 90\%$) of electric field by trapped electrons are canceled due to the image charges on the internal conductor. Although the exact profiles of plasmas after the stop of electron injection are not known at present, the image charge effect might lead to underestimate the trapped charge calculated from the frequency. The estimated charge is fairly consistent with the above-mentioned result from the Langmuir probe measurements. In the quiescent phase ($t = 0.7$ ms), we obtain $Q \sim 1 \times 10^{-8}$ C.

Figure 3(b) plots the charge on the wall probe as a function of time. The data were accumulated for many shots; each shot was artificially terminated by turning off the control electric potential V_{IC} , and the remaining charge on the wall probe was measured. In the initial phase ($t \leq 1$ ms), the charge decreases from 4.5×10^{-10} C to 1.4×10^{-11} C with a time constant of 1.3 ms. During the quiescent phase ($t \sim 2$ ms), we observe a much slower decay of the charge; the time constant of the decay is 0.2 s. Usually, the plasma confinement terminates with disruptive instability around $t \sim 0.1$ s (the time of disruption is referred to as “the lifetime”). Using the formula of the diffusion time due to neutral collisions [5] $\tau_D \approx \nu_{en}^{-1} \lambda_D^2 r_L^{-2}$ (ν_{en} , mean collision frequency; λ_D , Debye length; r_L , Larmor radius) and the experimental

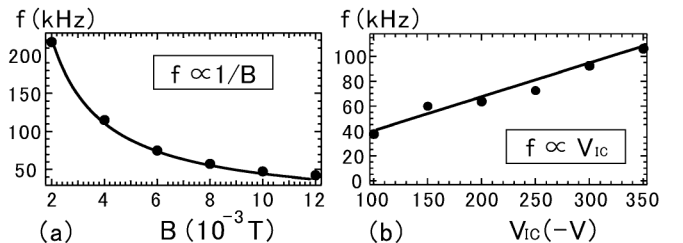


FIG. 4. The dominant frequency of electrostatic fluctuations (just before the quiescent phase) as functions of (a) the typical strength of dipole magnetic field B (at $r = 40$ cm) and (b) potential of the IC electrode V_{IC} . $P_{\text{base}} = 8 \times 10^{-5}$ Pa, (a) $V_{\text{IC}} = -250$ V, and (b) $B_{\text{typ}} = 6.0 \times 10^{-3}$ T.

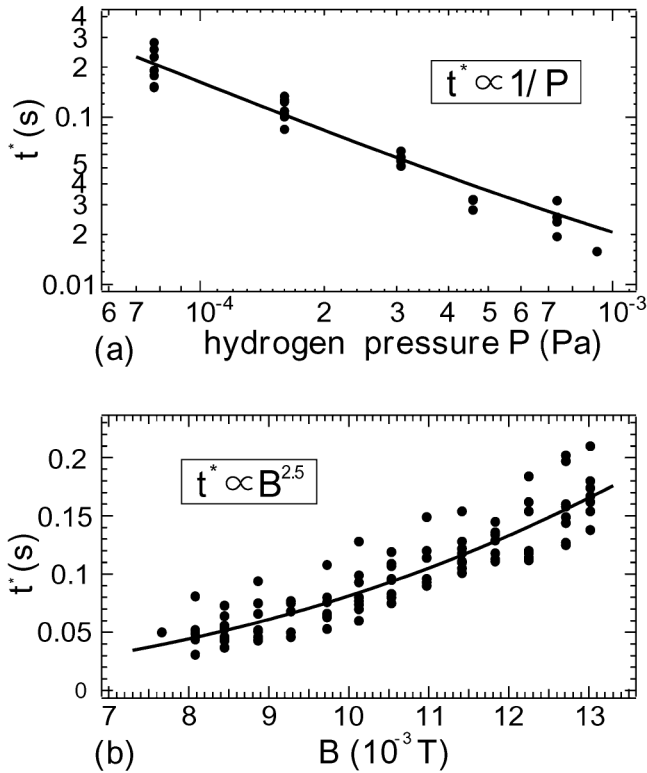


FIG. 5. The lifetime t^* as functions of (a) the back pressure of hydrogen gas and (b) typical magnetic field strength B . $P_{\text{base}} = 8 \times 10^{-5}$ Pa, (a) $B_{\text{typ}} = 1.3 \times 10^{-2}$ T, and (b) $V_{\text{IC}} = -300$ V.

parameters $B \sim 0.01$ T, electron temperature ~ 1 eV, and a density of $n_e \sim 10^{12} \text{ m}^{-3}$, we estimate $\tau_D \approx 0.1$ s. The classical diffusion time τ_D is comparable to the experimental results of both “lifetime” and decay time of the charge. The lifetime t^* varies as a function of the background pressure (P) and the magnetic field (B), suggesting the limit of the present confinement time is set by the effects of neutral collisions. We observe $t^* \propto P^{-1} B^{2.5}$, as shown in Fig. 5, and the use of higher vacuum and increase of the magnetic field strength would make possible the further longer confinement of electron plasmas. While the confinement time is close to the classical diffusion time, the scaling of the lifetime t^* shows a difference from the simple classical diffusion relation ($\propto P^{-1} B^2$), suggesting the onset of some instability (such as the ionization instability). Detailed analysis of fluctuations and scaling laws will be reported elsewhere.

In summary, we have demonstrated the long-term stable confinement of a toroidal electron plasma in a magnetic-surface configuration. In the initial fluctuating phase, the trapped charge adjusts (diminishes) to enter a quiescent phase. In the present device, we confined electrons with a peak density of an order of 10^{12} m^{-3} and

total charge of an order of $\sim 10^{-8}$ C for more than 0.1 s. The confinement time is limited by the collisional effects of the electrons with the remaining neutral gas. The realized confinement configuration would be important as for the applications for the advanced traps of charged particles such as positron-electron plasmas [16], as well as for the understanding of physical mechanism of plasma equilibria.

This work was supported by a Grant-in-Aid for Scientific Research (14102033) from MEXT Japan. The work of H. S. was supported in part by JSPS.

*Electronic address: saito@ppl.k.u-tokyo.ac.jp

- [1] W. Paul, Rev. Mod. Phys. **62**, 531 (1990).
- [2] S. J. Gilbert *et al.*, Phys. Rev. Lett. **88**, 043201 (2002).
- [3] M. Amoretti *et al.*, Nature (London) **419**, 456 (2002).
- [4] D. H. E. Dubin and T. M. O’Neil, Rev. Mod. Phys. **71**, 87 (1999).
- [5] J. H. Malmberg and C. F. Driscoll, Phys. Rev. Lett. **44**, 654 (1980).
- [6] J. D. Daugherty and R. H. Levy, Phys. Fluids **10**, 155 (1967).
- [7] L. Turner, Phys. Fluids B **3**, 1355 (1991).
- [8] K. Avinash, Phys. Fluids B **3**, 3226 (1991).
- [9] J. D. Daugherty, J. E. Eninger, and G. S. Janes, Phys. Fluids **12**, 2677 (1969).
- [10] W. Clark *et al.*, Phys. Rev. Lett. **37**, 592 (1976).
- [11] P. Zaveri *et al.*, Phys. Rev. Lett. **68**, 3295 (1992).
- [12] S. S. Khirwadkar *et al.*, Phys. Rev. Lett. **71**, 4334 (1993).
- [13] M. R. Stoneking *et al.*, Phys. Plasmas **9**, 766 (2002).
- [14] Z. Yoshida and H. Saitoh, in *Non-Neutral Plasma Physics IV*, edited by F. Anderegg, L. Schweikhard, and C. F. Driscoll (American Institute of Physics, New York, 2002), p. 703.
- [15] Z. Yoshida *et al.*, in *Nonneutral Plasma Physics III*, edited by John J. Bollinger, Ross L. Spencer, and R. C. Davidson (American Institute of Physics, New York, 1999), p. 397; Y. Ogawa *et al.*, in *Non-Neutral Plasma Physics IV* (Ref. [14]), p. 691.
- [16] T. S. Pedersen and A. H. Boozer, Phys. Rev. Lett. **88**, 205002 (2002).
- [17] H. Saitoh, Z. Yoshida, and C. Nakashima, Rev. Sci. Instrum. **73**, 87 (2002).
- [18] S. Kondoh and Z. Yoshida, Nucl. Instrum. Methods Phys. Res., Sect. A **382**, 561 (1996).
- [19] C. Nakashima *et al.*, Phys. Rev. E **65**, 036409 (2002).
- [20] C. Nakashima and Z. Yoshida, Nucl. Instrum. Methods Phys. Res., Sect. A **428**, 284 (1999).
- [21] R. H. Levy, J. D. Daugherty, and O. Buneman, Phys. Fluids **12**, 2616 (1969).
- [22] A. J. Peurrung, J. Notte, and J. Fajans, Phys. Rev. Lett. **70**, 295 (1993).